International Journal of Mass Spectrometry 195/196 (2000) 85–99

Dissociation chemistry of the hydrogen-bridged radical cation [CH$_2$=O $\cdots$ H $\cdots$ O=C–OCH$_3$]$^{\cdot+}$: proton transport catalysis and charge transfer

Lorne M. Fell[a], Paul J.A. Ruttink[b], Peter C. Burgers[c], Moschoula A. Trikoupis[a], Johan K. Terlouw[a,]*

[a]Department of Chemistry, McMaster University, Hamilton, Ontario L8S 4M1, Canada
[b]Theoretical Chemistry Group, Department of Chemistry, University of Utrecht, Padualaan 14, 3584 CH Utrecht, The Netherlands
[c]Hercules European Research Center BV, P.O. Box 252, 3770 AG Barneveld, The Netherlands

Received 10 May 1999; accepted 6 July 1999

Abstract

Tandem mass spectrometry based experiments on the decarbonylation products of ionized methyl-β-hydroxypyruvate (MHP) and dimethyloxalate (DMO) show that the hydrogen-bridged radical cation (HBRC) CH$_2$=O $\cdots$ H $\cdots$ O=C–OCH$_3^{\cdot+}$ is a stable species in the gas phase. Its low energy dissociation products are protonated methylformate, HOC(H)OCH$_3^+$, and the formyl radical, HC=O$^\cdot$. The HBRC isomers HOCH$_2$C(=O)OCH$_3^{\cdot+}$ (ionized methylglycolate) and (CH$_3$O)$_2$C=O$^{\cdot+}$ (ionized dimethylcarbonate) show the same dissociation characteristics. Deuterium labeling experiments dictate that loss of HC=O$^\cdot$ from the title HBRC cannot be formulated as a simple H shift from the formaldehyde moiety to the C atom of the O=C$^\cdot$–OCH$_3$ group. Ab initio molecular orbital (MO) calculations support the proposal that this dissociation proceeds via sequential transfers of a *proton, electron,* and another *proton* within ion–dipole complexes. The first step in this rearrangement process is a 1,2-proton shift catalyzed by a formaldehyde dipole. This yields an ion/dipole complex, CH$_2$=O $\cdots$ H–C(=O)OCH$_3^{\cdot+}$, that is in the correct configuration for electron transfer to occur at the energetic threshold dictated by experiment. The resulting intermediate triggers the transfer of yet another proton from the formaldehyde unit, thereby generating another stable H-bridged radical cation viz. HC=O $\cdots$ H $\cdots$ OC(H)OCH$_3^{\cdot+}$. This final intermediate dissociates with little or no activation energy into HOC(H)OCH$_3^+$ and HC=O$^\cdot$. It is further predicted by the calculations that ionized methylglycolate isomerizes into the title HBRC by a fairly high barrier that makes the communication between ionized methylglycolate and dimethylcarbonate via the title ion quite unlikely; instead an alternative route for this communication is proposed. (Int J Mass Spectrom 195/196 (2000) 85–99) © 2000 Elsevier Science B.V.

Keywords: Ab initio calculations; Ion-neutral complexes; Dimethyloxalate; Decarbonylation

1. Introduction

In a previous study the decarbonylation of ionized β-hydroxypyruvic acid (HPA) was investigated and it was shown that the high energy molecular ions dissociate into the hydrogen-bridged radical cation (HBRC) CH$_2$=O $\cdots$ H $\cdots$ O=C–OH$^{\cdot+}$ [1]. It was further reported that the methyl ester of HPA also readily decarbonylates upon ionization and it was tentatively proposed that the methyl substituted HBRC CH$_2$=O $\cdots$ H $\cdots$ O=C–OCH$_3^{\cdot+}$ was the product ion

---

* Corresponding author. E mail: terlouwj@mcmaster.ca
Dedicated to the memory of Professor Robert R. Squires.

PII S1387-3806(99)00137-2

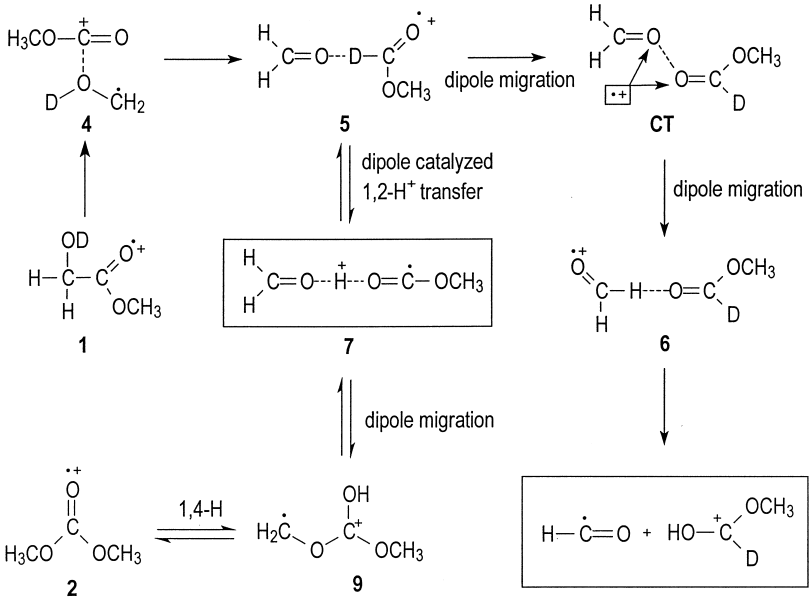

Scheme 1.

generated in the ion source. This interesting ion belongs to the *m/z* 90, $C_3H_6O_3^{\cdot+}$ family of ions that includes ionized methyl glycolate, $HOCH_2C(=O)OCH_3^{\cdot+}$, **1** and ionized dimethyl carbonate, $CH_3OC(=O)OCH_3^{\cdot+}$, **2**. The ion chemistry of **1** and **2** has been studied before and it was found that their low energy (metastable) ions predominantly lose a formyl radical, $HC{=}O^{\cdot}$, to yield $CH_3OC(H)OH^+$, protonated methylformate, as the product ion [2]. The kinetic energy releases (KER) as well as the dissociation levels for the two ions were found to be the same within experimental error and this was taken as evidence that **1** and **2** lose $HC{=}O^{\cdot}$ via the same mechanism. From extensive labeling experiments it was further concluded that **1** and **2** are separated by a sizable energy barrier and that **2** dissociates via **1** and not vice versa. Ab initio calculations were also performed, at the MP3/6-311G**/HF/6-31G** level of theory, and from experiment and theory a mechanism was derived that is presented in Scheme 1. In this mechanism the title HBRC $CH_2{=}O \cdots H \cdots O{=}C{-}OCH_3^{\cdot+}$, denoted as structure **7**, is proposed to be a key intermediate in the dissociation chemistry of low energy ions **1** and **2**.

We were curious then to see if **7** behaved analogously to ionized methylglycolate and indeed, in the metastable time frame it, too, readily loses $HC{=}O^{\cdot}$, with the same KER as **1** and **2**. Thus, the mechanism by which the HBRC loses $HC{=}O^{\cdot}$ may well be related to that of ions **1** and **2** and a detailed computational analysis of this mechanism forms the theme of this article.

A key experimental result from the previous study of **1** and **2** was that OD labeled ions **1** lose $HC{=}O^{\cdot}$ to produce the following C-D labeled product ion [2]:

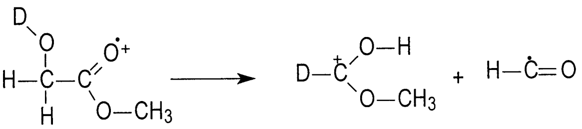

From extensive D, ^{13}C, and ^{18}O labeling experiments, it was further concluded that this reaction is 75% atom specific for ions **1**. The D labeled isotopomer $CH_2{=}O \cdots D \cdots O{=}C{-}OCH_3^{\cdot+}$ of **7** produces the same C-D labeled protonated methylformate ion as shown above for **1**-OD, but with an even higher atom specificity. This specific deuterium transfer eliminates many otherwise plausible mechanisms for the loss of HC=O$^{\cdot}$.

One mechanism that does satisfy the D labeling results in **1** involves conversion of the methylglycolate ion to its more stable enol counterpart, viz:

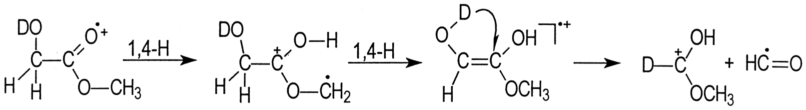

However, the dissociation chemistry of the enol ion appears to be quite different from that of the keto ion **1** [3], showing that enolization of **1** as proposed above does *not* occur.

A more plausible mechanistic proposal considered in [1] involves a mechanism akin to that for the loss of HC=O$^{\cdot}$ from ionized acetol [4a], $CH_3C(=O)CH_2OH^{\cdot+}$, and ethanediol [4b], $HOCH_2CH_2OH^{\cdot+}$, which features the concept of proton transport catalysis with electron transfer [4c] in hydrogen-bridged intermediates [4d]. For ions **1** the first step in this mechanism involves a 1,4-H transfer of the hydroxylic hydrogen to the ester's carbonyl group with concomitant C–C cleavage to form the HBRC **7**:

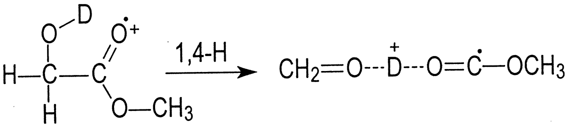

However, it was suggested in [1] that ion **7** cannot be generated directly from **1**: the computations indicated that migration of the hydroxyl hydrogen to the keto oxygen is not accompanied by C–C cleavage but rather leads to the unreactive stable distonic ion **8**, via a low lying transition state:

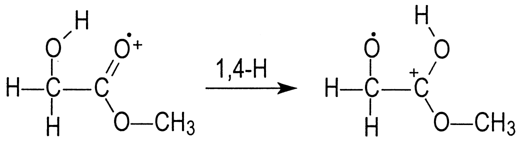

1 **8**

As an alternative, the mechanism of Scheme 1, which still features the concepts of dipole-catalyzed proton shift cum charge (electron) transfer, was proposed. Starting from methylglycolate ions, **1**, elongation of the C–C bond yields the ion–dipole complex **4**. Once generated, the $^{\cdot}CH_2OH$ dipole rotates and donates the hydroxylic hydrogen to the methoxycarbonyl cation to generate the high energy C–H $\cdots$ O bridged ion **5**. In this intermediate the formaldehyde dipole was proposed to move around the ionized methylformate and orient itself such that charge transfer occurs without affecting the total energy of the system [4b]. Because it is now charged, the CH_2=O moiety can rotate along the dipole vector of the O=C$^{\cdot}$–OCH_3 radical, to produce the C–H $\cdots$ O bridged ion **6**. This final intermediate can smoothly donate a proton to the $CH_3OC(H)$=O part leading to the low energy product ion $CH_3OC(H)OH^+$. As already mentioned, our HBRC CH_2=O $\cdots$ H $\cdots$ O–$OCH_3^{\cdot+}$ also figures in this proposal (ion **7** in Scheme 1), not as an intermediate en route to the dissociation of **1** but rather as a link between ions **1** and **2**.

Although ion **4** could not be identified as a stable minimum in the calculations in [1], it was argued that this ion–dipole complex would be sufficiently low in energy to be able to participate as a connecting intermediate in the generation of ion **5**. However, a recent reevaluation of the combined heats of formation of the ion–dipole components of **4**, $CH_3OC{=}O^+$, and $^{\cdot}CH_2OH$ leads to a value for $\Sigma\Delta H_f[CH_3OC{=}O^+ + {}^{\cdot}CH_2OH]$ that is 11 kcal mol^{-1} higher than that used in [1].* Hence the conversion of **1** into **4** is much more energy demanding than originally proposed and considering the low energy requirement for the

---

* ΔH_f^{total} changes from 114 to 125 kcal mol^{-1}, because $\Delta H_f(CH_2OH^{\cdot}) = -6$ kcal mol^{-1} [5a] has been revised to -4 kcal mol^{-1} [5b] and $\Delta H_f(CH_3OC{=}O^+) = 120$ kcal mol^{-1} [5a] becomes 129 kcal mol^{-1} [5c].

$HC{=}O^{\cdot}$ loss, ~12 kcal mol^{-1}, the route **1** → **4** → **5** becomes unlikely. It is one of the goals of this article to further investigate this part of the reaction mechanism and in particular to reexamine the feasibility of the isomerization **1** → **7** discussed above at a higher (correlated) level of theory.

The 25% nonatom specific loss of $HC{=}O^{\cdot}$ from **1** was proposed to originate from a partial interconversion with ions **2**, whose D-labeled isotopomers quickly lose their positional identity because of a facile interconversion with the very stable distonic ions **9** and **9′** via 1,4-H and 1,5-H shifts, viz.

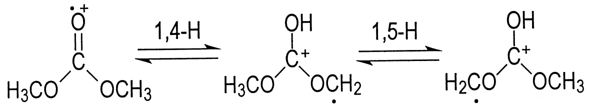

2 **9** **9'**

However, both the loss of $HC{=}O^{\cdot}$ from **2** and the nonspecific loss of $HC{=}O^{\cdot}$ from **1** were proposed to occur via the mechanism proposed for the specific loss of $HC{=}O^{\cdot}$ from **1**, as outlined in Scheme 1. Note that there is solid experimental evidence for the proposal that **1** and **2** lose $HC{=}O^{\cdot}$ via a single common dissociation route but the problematic part in Scheme 1 is that it is our HBRC **7** that is supposed to form the link in the communication between **1** and **2**. It was argued in [1] that **7** could fulfill this role because the calculations had shown that the HBRC is best represented as $CH_2{=}O \cdots H{-}O{-}C{-}OCH_3^{\cdot+}$, which is a methoxy-hydroxycarbene ion interacting with the formaldehyde dipole, and in such a species one can indeed envisage a facile $CH_2{=}O$ migration to generate ion **9**. However, this proposal implies that the HBRC exhibits a higher degree of nonspecific D/H exchange than **1**. This is clearly not the case (see below) and thus ion **7** is *not* the connecting intermediate between **1** and **2** and there must be another route for the conversion **2** → **1**. We reiterate that a relatively high barrier must separate **1** (and **7**) from **2** to allow for the atom specific $HC{=}O^{\cdot}$ loss from **1**.

In summary, the experimental identification and characterization of the HBRC **7** questions some aspects of the mechanistic proposal presented in Scheme 1 and we have therefore investigated selected parts of this potential energy surface with calculations at a more advanced level of theory. In the first part of Sec. 2, the experimental findings on the identification and the dissociation of the new HBRC **7** will be reviewed. In the second part of the section the computational results of the process **7** → $HC{=}O^{\cdot}$ + $CH_3OC(H)OH^+$ are presented and it will be shown that they support the proposal that ions **7** dissociate via a catalyzed 1,2-H^+ shift, an electron transfer between moieties, and a final spontaneous proton transfer. In Sec. 2.3, it will be shown that **1** can isomerize into **7** prior to loss of $HC{=}O^{\cdot}$, via the sequence **1** → **7** → **5** → **CT** → **3/6** → products, and that this pathway is more likely than that proposed previously [2], i.e. **1** → **4** → **5** → **CT** → **6** → products, see Scheme 1. This section also deals with a tentative new proposal for the communication between **1** and **2** that accounts for the partial H/D exchange in D-labeled isotopomers of **1**.

2. Results and discussion

2.1. Experimental observations on the HBRC $[CH_2{=}O \cdots H \cdots O{=}C{-}OCH_3]^{\cdot+}$

We will begin our discussion with the experimental identification of $CH_2{=}O \cdots H \cdots O{=}C{-}OCH_3^{\cdot+}$. The electron ionization (EI) mass spectra of methyl-β-hydroxypyruvate (MHP), $HOCH_2C({=}O)COOCH_3$, and dimethyloxalate (DMO) $CH_3OC({=}O)C({=}O)OCH_3$, both exhibit an interesting rearrangement product ion at *m/z* 90 corresponding to $C_3H_6O_3^{\cdot+}$ [1,6]. This *m/z* 90 ion* results from a decarbonylation of the molecular ions: from MHP this likely occurs via formation of an intramolecular H bond and C–C cleavage followed by loss of the keto CO moiety [1] and from DMO via a 1,5-H shift and $CH_2{=}O$ migration [6], as depicted in Scheme 2.

The CID mass spectra [10 keV ions, collision gas O_2] of the product ions from these two decarbonylation processes are identical and the spectrum obtained

---

* For MHP and DMO the ions comprise 70% and 0.5% of the base peak at *m/z* 59, respectively.

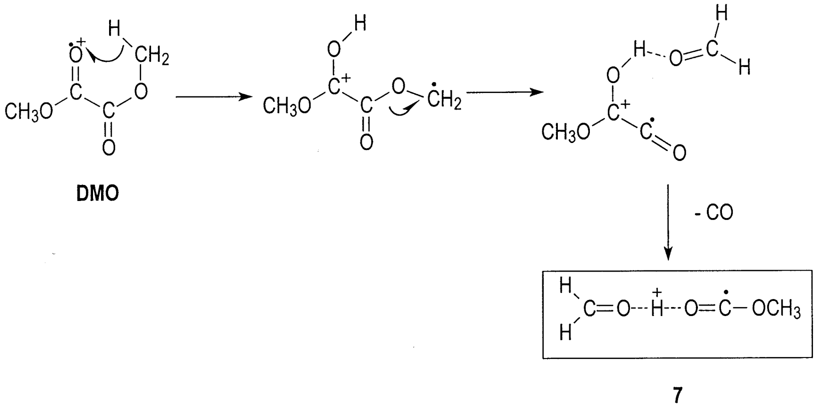

Scheme 2.

using DMO as the precursor molecule is presented in Fig. 1(a). It features intense signals at *m/z* 31, CH_2OH^+, and *m/z* 60, $CH_3OCOH^{\cdot +}$ (the carbene's structure was identified from a double collision experiment, result not shown) of almost equal intensity and considering the very similar proton affinities of $CH_3OC{=}O^{\cdot}$ and $CH_2{=}O$ (168 and 170 kcal mol^{-1}, respectively[†]) this is precisely what is expected for the proposed HBRC $CH_2{=}O \cdots H \cdots O{=}C–OCH_3^{\cdot +}$. A closely similar collision-induced dissociation (CID) mass spectrum, see Fig. 1(b), was obtained for the decarbonylation product of the *metastable* DMO ions [third field-free region (3ffr) CID spectrum of 10 keV metastable precursor ions dissociating in the second field-free region (2ffr) of the instrument] and this strengthens our proposal that we are dealing with a single ion structure.

Fig. 1(c) and (d) present the CID mass spectra of the isomeric methylglycolate ions, $HOCH_2C({=}O)OCH_3^{\cdot +}$, **1**. Fig. 1(d) represents the conventional CID spectrum. It is dominated by the *m/z* 61 peak but almost all of the $CH_3OC(H)OH^+$ ions represented by this signal originate from spontaneous (metastable) dissociations rather than collision induced processes. In fact, the fraction of the stable ions **1** that is metastable is remarkably high (~10%). We have therefore recorded a more representative CID spectrum of **1**, which is presented in Fig. 1(c) [this spectrum was obtained by applying a voltage (+1000 V) on the collision gas chamber to separate the metastable *m/z* 61 ions from the CID generated ions and by deleting the metastable peak from the recorded spectrum]. It is seen that the CID characteristics of **1** and **7** are similar but nonetheless distinctly different. Note in particular the decreased *m/z* 60 and the increased *m/z* 59 intensities in the spectrum of **1**, in keeping with the differences in structure of the two ions.

In contrast, the metastable ion (MI) spectra of ions **1** and **7** are virtually identical: both ions predominantly lose $HC{=}O^{\cdot}$ with the same kinetic energy release ($T_{0.5}$ = 23 meV) to yield the same product ion, $CH_3OC(H)OH^+$, whose structure was established from a double collision experiment. Moreover, the D labeled isotopomers $DOCH_2C({=}O)OCH_3^{\cdot +}$ and $CH_2{=}O \cdots D \cdots O{=}C–OCH_3^{\cdot +}$ (generated from $DOCH_2C({=}O)COOCH_3$) both yield the same D labeled product ion $CH_3OC(D)OH^+$ with a high degree of atom specificity. Fig. 1(e) shows the CID spectrum of the metastably generated *m/z* 62 product ions generated by loss of $HC{=}O^{\cdot}$ from $CH_2{=}O \cdots D \cdots O{=}C–OCH_3^{\cdot +}$ and comparison with the reference spectrum (Fig. 1(b) in [1]) leaves no doubt that the ions have the $CH_3OC(D)OH^+$ structure. Thus it is indeed likely that metastable ions **1** and **7** lose $HC{=}O^{\cdot}$ via the same mechanism and consider-

---

[†] From $CH_3OC{=}O^{\cdot} + H^+ \rightarrow CH_3OCOH^{\cdot +}$ + PA, using $\Delta H_f(CH_3OC{=}O^{\cdot}) = -40$ kcal mol^{-1} [7] and $\Delta H_f(CH_3OCOH^{\cdot +}) = 158$ kcal mol^{-1} [5a]; PA ($CH_2{=}O$) from [5d].

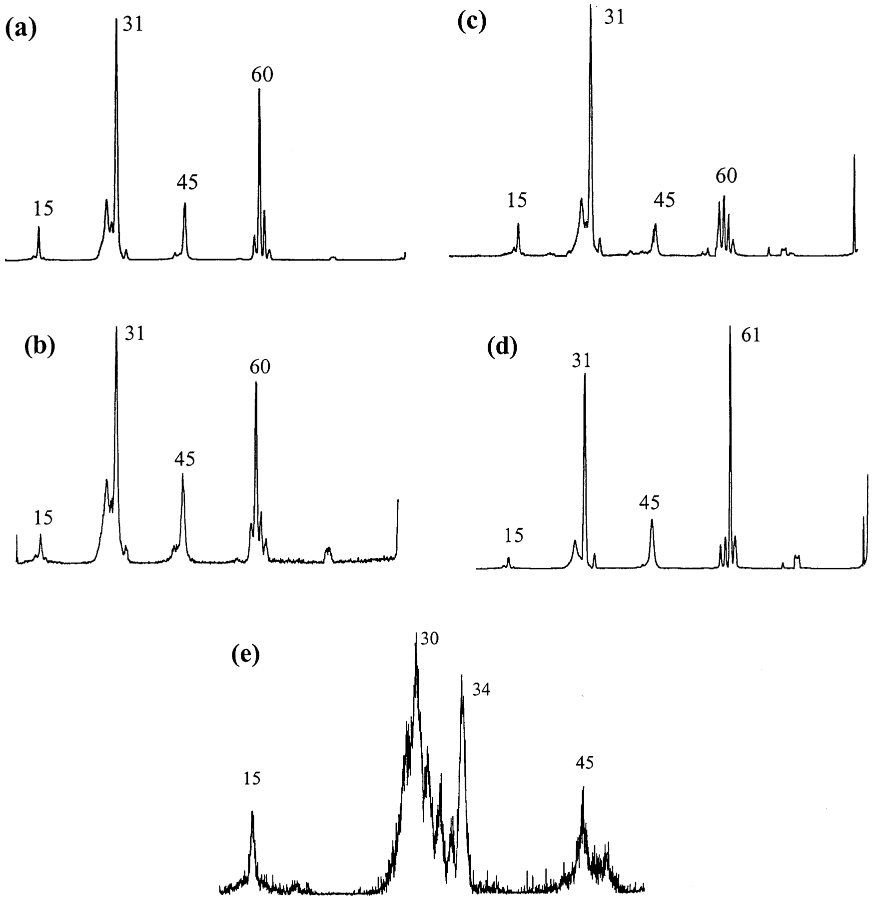

Fig. 1. CID mass spectra of (a) the (8 keV) source generated $[M–CO]^{\cdot+}$ ions $CH_2=O \cdots H \cdots O=C–OCH_3^{\cdot+}$ from dimethyloxalate; (b) the $[M–CO]^{\cdot+}$ ions generated from metastable (10 keV) dimethyloxalate ions; (c) source generated (8 keV) methylglycolate ions, $HOCH_2COOCH_3^{\cdot+}$, with the dominating metastable peak at *m/z* 61 removed, see text; (d) source generated (8 keV) methylglycolate ions, uncorrected spectrum; (e) the $CH_3OC(D)OH^+$ ions generated from metastable ions $CH_2=O \cdots D \cdots O=C–OCH_3^{\cdot+}$, formed by the decarbonylation of OD labeled methyl-β-hydroxypyruvate, $DOCH_2C(=O)COOCH_3^{\cdot+}$.

ing the arguments presented in the Introduction, the dissociation route **1** → **7** → **5** → **CT** → **6** → products is the most promising candidate for computational analysis. We further note that the reaction sequence **1** → **7** → products is more plausible than any route **7** → **1** → products and that there must be a sizable barrier for the isomerization **1** → **7**. This is because the degree of atom specificity in the loss of HC=O$^\cdot$ from isotopomers of **1** is fairly high but nevertheless lower than that observed from isotopomers of **7** (cf. $DOCH_2C(=O)OCH_3^{\cdot+}$ and $CH_2=O \cdots D \cdots O=C–OCH_3^{\cdot+}$ for which the ratio of loss of HC=O$^\cdot$ versus DC=O$^\cdot$ are 97:3 and 98:2, respectively, whereas $DOCH_2C(=O)OCD_3^{\cdot+}$ and $CH_2=O \cdots D \cdots O=C–OCD_3^{\cdot+}$ yield ratios of 83:17 and 88:12, respectively). One final experimental observation deserves to be mentioned: for the loss of HC=O$^\cdot$ from ions **1** and **2** it could be established (from appearance energy measurements, see [2]) that the highest transition state (TS) in any proposed mechanism* should lie at ~12 kcal mol^{-1} above the dissociation products

---

* From AE (*m/z* 61) [**1**] = 10.74 ± 0.05 eV and ΔH_f [**1**] = −133.1 kcal mol^{-1} [8a], AE (*m/z* 61) [**2**] = 10.94 ± 0.05 eV and ΔH_f [**2**] = −136.5 kcal mol^{-1} [8b] and using $\Sigma \Delta H_f$ (products) = 103 kcal mol^{-1}, see Table 1, footnote f.

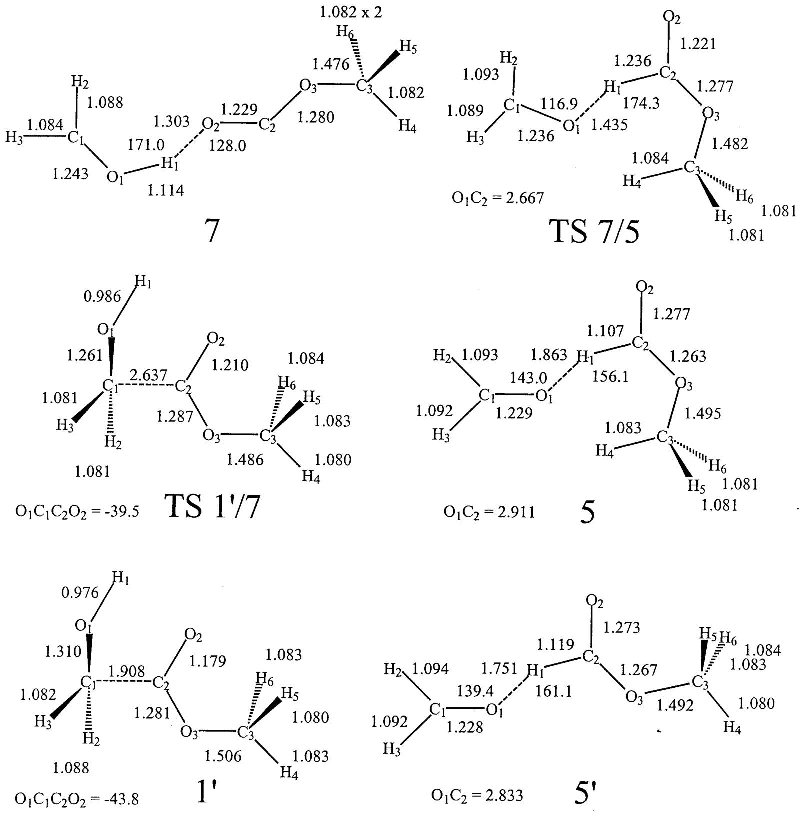

Fig. 2. The UMP2(Full)/6-31G** optimized geometries for the HBRC **7** and its key isomers and transition states. The geometry for CT was calculated at the UHF/6-31G* level of theory, see text. Structures labeled "EF" were located with an eigenvalue-following routine, see Sec. 3.

$CH_3OC(H)OH^+$ and $HC{=}O^{\cdot}$. For ions **7** no such experimental observations are available but, if it is indeed a key intermediate in the dissociation chemistry of **1** and **2**, this energetic constraint applies to its dissociation too.

2.2. Loss of $HC{=}O^{\cdot}$ from ion 7, $CH_2{=}O \cdots H \cdots O{=}C{-}OCH_3^{\cdot+}$: computational evidence for the double proton and single electron transfer mechanism

Our calculations confirm the proposal derived from the experiments that ion **7** is a stable species in the gas phase. From a standard population analysis on its optimized structure presented in Fig. 2, it follows that the ion is best described as a CH_2OH^+ ion interacting via a H bridge with the $CH_3OC{=}O^{\cdot}$ dipole. The bridging H atom is closer to the $CH_2{=}O$ moiety than the $CH_3OC{=}O^{\cdot}$ component and this is in line with the observation that the proton affinity (PA) of $CH_2{=}O$ is higher than that of $CH_3OC{=}O^{\cdot}$, albeit by only 2 kcal mol^{-1}. This may explain why ion **7**'s UHF optimized geometry [2] is found to have the bridging H attached to the methoxycarbonyl moiety, viz. $CH_2{=}O \cdots H{-}O{-}C^{\cdot+}{-}OCH_3$. It seems likely that little energy is required to shift the bridging H between the two moieties and that at the level where the HBRC undergoes isomerization, it can adopt either charge distribution. From the results in Table 1, it follows that the ion is stabilized by 33 kcal mol^{-1} relative to the dissociation products **C**, from which we derive ΔH_f (**7**) = 95 kcal mol^{-1}, in excellent agreement with an empirical estimate [10].

A 1,2-proton shift in HBRC **7** yields the C–H–O

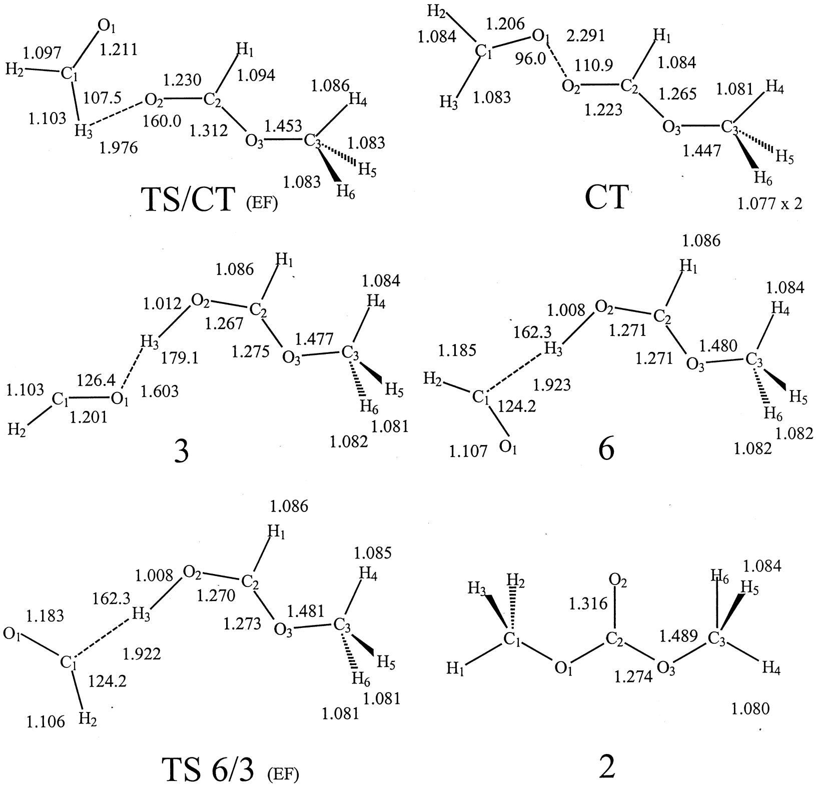

Fig. 2. *(continued)*

bridged ion **5** via **TS 7/5**, whose MP2 energy (see Table 1) lies only slightly above that of the connecting ion **5**. Note also that the optimized geometries for **5** and **TS 7/5** are closely similar: the only significant difference lies in the position of the bridging H relative to the connecting moieties. When single point calculations are performed to obtain better relative energies, both the energy of **5** and that of **TS 7/5** are lowered to such an extent that the resulting values (15 and 11 kcal mol^{-1}, respectively; see Table 1) are now compatible with the ~12 kcal mol^{-1} derived from experiments for the highest point along the reaction coordinate. Unfortunately, in the single point calculations the energy of **TS 7/5** becomes lower than that of the connecting ion **5**. This is an imperfection in the methodology used that probably stems from the fact that the MP2 optimized geometries of the two closely similar species are not sufficiently refined. The problem could be remedied by performing the geometry optimizations (and frequency calculations) at a higher level of theory [e.g. CCSD(T)], but considering the size and complexity of the system, such calculations are not yet feasible.

Nevertheless, it is clear that starting from ion **5**, which can be viewed as an ion–dipole complex between $CH_3OC(=O)H^{\cdot+}$ and $CH_2{=}O$, the 1,2-H transfer leading to **7** occurs with little or no activation energy. Viewing this reaction as the isomerization of $CH_3OC(=O)H^{\cdot+}$ into its more stable carbene isomer, $CH_3OCOH^{\cdot+}$, it follows that the $CH_2{=}O$ moiety in **5** is responsible for the effective removal of the high barrier associated with the unassisted isomerization. The ions $CH_3OC(=O)H^{\cdot+}$ [11(a)] and $CH_3OCOH^{\cdot+}$ [11(b)] have entirely different MI characteristics and from an analysis of their structure characteristic dissociation reactions it follows that the two isomers are separated by a 1,2-H shift barrier of at least 40 kcal mol^{-1}. For a closely related system, viz.

Table 1

The UMP2(Full)/6-31G(d, p) and CCSD(T)/cc-pVDZ//UMP2 energies (hartrees), scaled[a] zero-point vibrational energies (ZPVEs, kcal mol^{-1}) and relative energies, E_{rel} (kcal mol^{-1}) of the H-bridged ion $CH_2{=}O \cdots H \cdots O{=}C{-}OCH_3^{\cdot+}$ and its most important isomers and dissociation products

Species		ZPVE	MP2(Full) /6-31G(d, p) −342	E_{rel}	CCSD(T) /cc-pVDZ −342	E_{rel}	E_{rel} (+ ZPVE)	E_{rel} expt
$HOCH_2C({=}O)OCH_3^{\cdot+}$	**1′**	58.9	0.31134	−4.2	0.38616	−1.6	2.5	4[b]
$CH_3OC({=}O)OCH_3^{\cdot+}$	**2**	58.7	0.29882	3.6	0.38165	1.2	5.1	3[c]
$HC{=}O \cdots H \cdots OC(H)OCH_3^{\cdot+}$	**3**	57.2	0.32994	−15.9	0.40854	−15.6	−15.1	
$CH_2{=}O \cdots H{-}C({=}O)OCH_3^{\cdot+}$	**5**	55.9	0.27119	21.0	0.36131	14.0	15.1	
$CH_2{=}O \cdots H{-}C({=}O)OCH_3^{\cdot+}$	**5′**	55.4	0.26988	21.8	0.36099	14.2	14.7	
$^{\cdot+}O{=}C(H){-}H \cdots O{=}C(H)OCH_3$	**6**	56.4	0.32277	−11.4	0.40148	−11.2	−9.6	
$CH_2{=}O \cdots H \cdots O{=}C{-}OCH_3^{\cdot+}$	**7**	55.6	0.31280	−5.1	0.39068	−4.4	−3.6	
$CH_2{=}O^{\cdot+} \cdots O{=}C(H)OCH_3$	**CT-1**		0.26090	27.4	0.36266	13.2		
$CH_2{=}O \cdots {}^{\cdot+}O{=}C(H)OCH_3$	**CT-2**		0.26369	25.7	0.36298	13.0		
TS-CT (see text)	**TS/CT**	55.3	0.26718	23.5	0.36305	12.9	13.4	
	TS 7/5	53.2	0.26515	24.8	0.36415	12.3	10.6	
	TS 1/7	57.2	0.28985	9.3	0.36823	9.7	12.1	
	TS 6/3[h]	56.4	0.31980	−9.5	0.39869	−9.4	−7.9	
$CH_2{=}O + HC({=}O)OCH_3^{\cdot+}$	**A**	54.5	0.24273	38.8	0.33169	32.6	32.2	35[d]
$CH_2{=}O + HOCOCH_3^{\cdot+}$	**B**	54.6	0.26154	27.0	0.34006	27.4	27.2	29[e]
$^{+}CH_2OH + CH_3OC{=}O^{\cdot}$	**C**	55.8	0.25905	28.6	0.33886	28.1	29.1	25[f]
$HC{=}O^{\cdot} + HOC(H)OCH_3^{+}$	**D**	54.9	0.30463	0.0	0.38369	0.0	0.0	0[g]

[a] Scaled by a factor of 0.9646 (see [9]).

[b] Using ΔH_f (**1**) = 107 ± 2 kcal mol^{-1}, from ΔH_f (ester) = −133.1 ± 1.5 kcal mol^{-1} [8a] and IE (ester) = 10.42 ± 0.05 eV [2].

[c] ΔH_f (**2**) = 106 ± 2 kcal mol^{-1}, from [2] but using a revised value for ΔH_f (ester) = −136.5 ± 1.5 kcal mol^{-1} [8b].

[d] Using ΔH_f^{total} = 138.4 kcal mol^{-1}, from ΔH_f ($CH_2{=}O$) = −26.0 kcal mol^{-1} [5a] and ΔH_f ($CH_3OC(H){=}O^{\cdot+}$) = 164.4 kcal mol^{-1} [5a].

[e] Using ΔH_f^{total} = 132.0 kcal mol^{-1}, from ΔH_f ($CH_2{=}O$) = −26.0 kcal mol^{-1} [5a] and ΔH_f ($CH_3OCOH^{\cdot+}$) = 158 kcal mol^{-1} [5a].

[f] Using ΔH_f^{total} = 128 kcal mol^{-1}, from ΔH_f (CH_2OH^+) = 168 kcal mol^{-1} [5a] and ΔH_f ($CH_3OC{=}O^{\cdot}$) = −40 kcal mol^{-1} [7].

[g] Using ΔH_f^{total} = 103 kcal mol^{-1}, from ΔH_f ($HC{=}O^{\cdot}$) = 10 kcal mol^{-1} [5b] and ΔH_f ($CH_3OC(H)OH^+$) = 93 kcal mol^{-1} [5a].

[h] IRC for **TS 6/3** not performed but imaginary vibrational frequency was geometrically analyzed.

$CH_3C({=}O)H^{\cdot+}$ and $CH_3COH^{\cdot+}$, this 1,2-H shift isomerization barrier has been recently calculated at the G2 level of theory as 37 kcal mol^{-1} [11(c)]. However, high level computational studies by Radom et al. [12(a)–(c)] and elegant experimental studies by Bohme et al. [13(a)] and Audier et al. [13(b)–(d)] have shown that the prohibitively high 1,2-H shift barrier for the unassisted isomerization in systems like $HCO^+ \rightarrow {}^+COH$ and $CH_3OH^{\cdot+} \rightarrow CH_2OH_2^{\cdot+}$ could be drastically lowered by interaction with a neutral base (B). For the transformation, it was found that efficient catalysis will take place [see Eq. (1)] when the PA of the base lies between the PA of [X–Y] at X and Y. If the PA [B] is significantly lower than the PA [XY] at Y, the first step in Eq. (1) will not take place

$$[H{-}X{-}Y]^{\cdot+} + B \rightarrow B \cdots H^{+} \cdots [X{-}Y] \rightarrow$$

$$B \cdots H^{+} \cdots [Y{-}X] \rightarrow B + [X{-}Y{-}H]^{\cdot+} \qquad (1)$$

If, on the other hand, PA [B] is significantly larger than PA [XY] at X, then the intermediate complex $B \cdots H^+ \cdots [X{-}Y]^{\cdot}$ will dissociate to $[X{-}Y]^{\cdot}$ and HB^+ via a unidirectional proton transfer. In effect, if PA[B] is intermediate, the barrier becomes negative relative to the separated reactants and products and the base successfully catalyzes the isomerization. In our case we are dealing with a base ($CH_2{=}O$) with a slightly higher PA than required for the catalysis; this, and the fact that it has a significant dipole moment, effects a facile catalysis but without separation of the base after the event.

Ion **5** (and its slightly more stable conformer **5′**) can indeed be viewed as a complex of the methylformate radical cation and a formaldehyde dipole. A standard population analysis indicates that the charge is largely located on the carbonyl moiety of the methylformate component of the optimized geometry shown in Fig. 2. It is further seen that the neutral formaldehyde is oriented towards the charge such that ion–dipole stabilization can occur. We further note from the computational results in Table 1, that **5** is stabilized relative to its components CH_2=O and $^{\cdot+}$O=C(H)OCH_3(**A**) by $\sim$17 kcal mol^{-1} and that the stabilization energy calculated from the classic ion–dipole interaction formula, $SE = 68.8\mu \cos\theta/r^2$ [$\mu(CH_2{=}O) = 2.33$ D, and deriving $r \sim 3.5$ Å and $\theta = 23°$ from the geometry in Fig. 2] yields 13 kcal mol^{-1}. Thus, apart from a conventional H bridge, there is indeed a sizable electrostatic interaction in this C–H–O bridged intermediate.

The next step in the dissociation mechanism involves a H transfer from the CH_2=O moiety to the O atom of the carbonyl group in methylformate. However, transfer of a $H^{\cdot}$ from the neutral CH_2=O molecule to the charged methylformate moiety in **5** is expected to be more energy demanding (see [4(a)]) than dissociation of the ion–dipole complex into its components $CH_3OC(H){=}O^{\cdot+}$ and CH_2=O. One of the possibilities that we have entertained to locate the TS for such a transfer involved an a priori plausible conformer of **5**, as the starting point, viz.

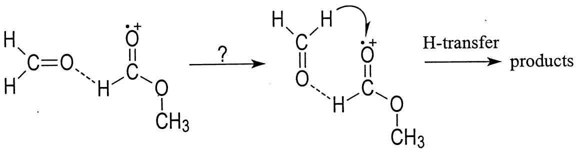

5″ 5‴

However, neither **5″** nor **5‴** represent minima on the PES and geometry optimizations starting from these structures yielded the stable conformer **5** depicted in Fig. 2, in which the CH_2=O moiety has moved away from the ionized C=O moiety of the methylformate. That ion **5′** is not a stable minimum on the PES is not so surprising if one considers that a potentially favourable ion–dipole interaction is counteracted by a strong repulsion between the lone pair electrons of the two O atoms.

By analogy with previous computational studies on related systems (loss of HC=$O^{\cdot}$ from ionized acetol and ethylene glycol [4]) we examined the possibility that the H is transferred as a proton, but this of course requires that the transfer be preceded by a charge transfer (CT) from the methylformate moiety to the formaldehyde molecule. Note that CT in this system may well be favourable because the components $CH_3OC(=O)H$ and CH_2=O have almost the same ionization energy (10.82 and 10.87 eV, respectively [5(a)]) and substantial dipole moments as well (1.77 and 2.33 D, respectively [2]). For reasons stated below, the feasibility of this charge transfer was first investigated at the unrestricted HF level of theory. UHF/6-31G* calculations yielded a minimum energy crossing point whose optimized geometry is presented in Fig. 2 as **CT**. Its energy was derived from single point calculations on two electronic configurations, listed in Table 1 as **CT-1** and **CT-2**. **CT-1** represents an ion of fixed **CT** geometry where the charge is positioned on the methylformate moiety, whereas in **CT-2** the charge is positioned on the formaldehyde unit. The resulting E_{rel} value, 13 kcal mol^{-1}, is gratifyingly close to that for ion **5**, thus supporting the proposal that the charge transfer is energetically feasible. When, starting from the **CT** geometry with the charge located on the formaldehyde moiety, the UHF/6-31G* energy is optimized, a minimum is reached represented by the C–H $\cdots$ O bridged ion $^{\cdot+}$O=C(H)–H $\cdots$ O=C(H)OCH_3, **6**, and from which a facile proton transfer to the dissociation products $CH_3OC(H)OH^+$ and HC=$O^{\cdot}$ may be expected to occur [2]. Starting from **CT-1** a connection with ion **5** was established (see below) and thus at the HF level of theory the route **5** → **CT** → products appears to be feasible.

Reverting to the UMP2 methodology we are using to examine this PES, we find a transition state **TS/CT** whose geometry is closely similar to that of **CT** but with the charge situated on the formaldehyde component. A structure optimization starting from this **TS/CT** geometry yielded the very stable HBRC **3**, HC=O $\cdots$ HO–C(H)$OCH_3^{\cdot+}$. This indicates that a facile proton transfer from the formaldehyde moiety in **TS/CT** to its methylformate component is feasible. Under the conditions imposed by the experiment, ion **3** generated upon charge transfer will only have a fleeting existence because its internal energy is such (see Fig. 3) that a fast dissociation into

$CH_3OC(H)OH^+$ and $HC{=}O^{\cdot}$ will occur by direct bond cleavage.

Although the optimization of **TS/CT** geometry spontaneously leads to ion **3**, we have also computationally identified the HBRC **6** as a low lying minimum on the PES. This HBRC (see Fig. 2) can be considered as C–H–O bridged intermediate between the dissociation products **D**, see Table 1. Ion **6** communicate with HBRC **3** via a low lying transition state, **TS 6/3**, and thus the exothermic dissociation step **CT** → **3** → products can also be envisaged as **CT** → **6** → products or **CT** → **6** → **3** → products. In fact, it is conceptually easier to picture the mechanism as **CT** → **6** → **3** → products but whether or not this sequence is preferred is not important here: at the elevated energies either **6** or **3** dissociates with little or no activation energy.

Establishing a connection between **TS/CT** and ion **5** appeared to be problematic. Structure optimizations starting from **TS/CT**-like geometries slightly distorted towards **5** were unsuccessful: the steps taken in this procedure tended to get smaller and smaller whereas the gradients remained sizable. The reason for this is that the Hessian becomes numerically unstable, leading to unreasonably large eigenvalues and therefore vanishingly small steps. This numerical instability may be caused by the fact that several UHF solutions coexist in this part of the PES. The wave function optimization uses the lowest possible UHF energy, but this does not always correspond to the lowest UMP2 energy. As a consequence it is difficult to find the minimum with the lowest UMP2 energy. If we start the UMP2 geometry optimization at the (UHF) **CT** geometry the calculation still does not converge because here too the character of the UHF wave function changes all the time. However, optimizing the UHF/6-31G* energy starting from the **CT** geometry with the charge located on the $CH_3OC(H){=}O$ moiety yields **5**. This reaction path was checked by doing UMP2/6-31G** single point calculations for several of the geometries encountered in the UHF geometry optimization. Because the UMP2 energies found in this way were lower than the UMP2 energy for the **CT-2**, the rate-determining step in this reaction is the passage of the **CT/TS** region.

Thus, we have good computational evidence for the occurrence of proton and electron transfers in this system and Fig. 3 summarizes our computational results in an energy level diagram that uses the dissociation level $CH_3OC(H)OH^+ + HC{=}O^{\cdot}$ as the anchor point. The hatched area in the figure represents the energy range where the first proton transfer and the charge transfer occur. The dissociation level derived from the experiment (12 kcal mol^{-1} relative to the anchor point, see Sec. 1) is also presented as a dashed line.

2.3. A new proposal for the isomerization 7 → 1 and the question of the communication between ions 1 and 2

In the previous section it was proposed, on the basis of ab initio calculations, that the dissociation of low energy HBRC ions **7** occurs via a dipole catalyzed 1,2-H^+ shift and a charge transfer followed by a spontaneous proton transfer, i.e. the sequence **7** → **5** → **CT** (→ **6**) → **3** → products **D**.

The first question addressed in this section is whether the methylglycolate ions **1** can also follow this route, i.e. isomerize via the sequence **1** → **7** → **5** → **CT** (→ **6**) → **3** → **D** as suggested in Sec. 1. As already mentioned, Suh et al. [2] suggested that ion **7** cannot be generated directly from **1** because the (UHF) computations on the 1,4-H shift involved in this process all led to a facile isomerization into the stable but unreactive distonic ion **8**. There is little doubt that this simple 1,4-H shift requires little or no activation energy. In fact, computational studies on ionized ethylene glycol [4] and glycolic acid [1] showed that optimizing the geometry of an initial guess conformer of conventional C–C bond length that has the hydroxylic H pointing to the adjacent O atom yielded a distonic ion via a "spontaneous" 1,4-H transfer. However, it was also found in these studies (and also in computational studies on ionized acetol [4] and 1,2-propanediol [14]) that one of the conformers of the ionized precursor molecule existed as a stable long C–C bonded (non-ion–dipole) species and that a 1,4-H shift starting from this conformer led to the formation of the O–H–O bridged ion. Five of the

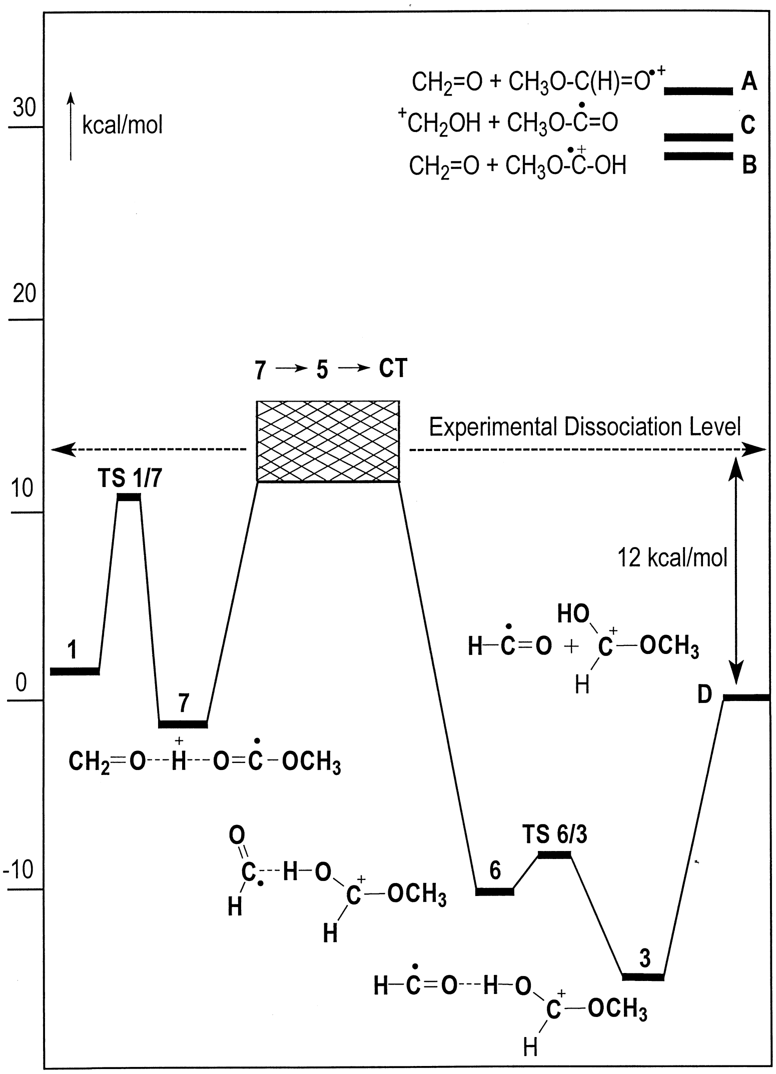

Fig. 3. Energy level diagram describing the dissociation of the HBRC **7** and the methylglycolate ion **1** as derived from ab initio calculations. The hatched area represents the energy range where the first proton and the charge transfer occur.

eight conformers of **1** were identified as stable minima in [1] (q.v. structures **1b**–**1h** in Fig. 3) but they are all characterized by a C–C bond of conventional length (~1.52 Å) and a hydroxylic H that points away from the carbonyl O atom. This is not to say that a stable long-bonded conformer of **1** does not exist, but one possibility is that the UHF level of theory employed in [1] is not adequate to describe such a species as a stable minimum. In any case, we decided to search for such a species at the more advanced UMP2 level of theory using an initial guess in which the distance between the central carbon atoms was large, ~2 Å, and that had the hydroxyl H pointing towards the keto oxygen. This geometry optimization led to the minimum **1′** in Fig. 2 that is characterized by both a long C–C bond (1.91 Å) and a hydroxylic H pointing to the carbonyl O atom.

Starting from this structure, it was fairly straightforward to find the elusive connection between ions **1** and **7** that is represented by **TS 1/7**, in Fig. 2. This TS,

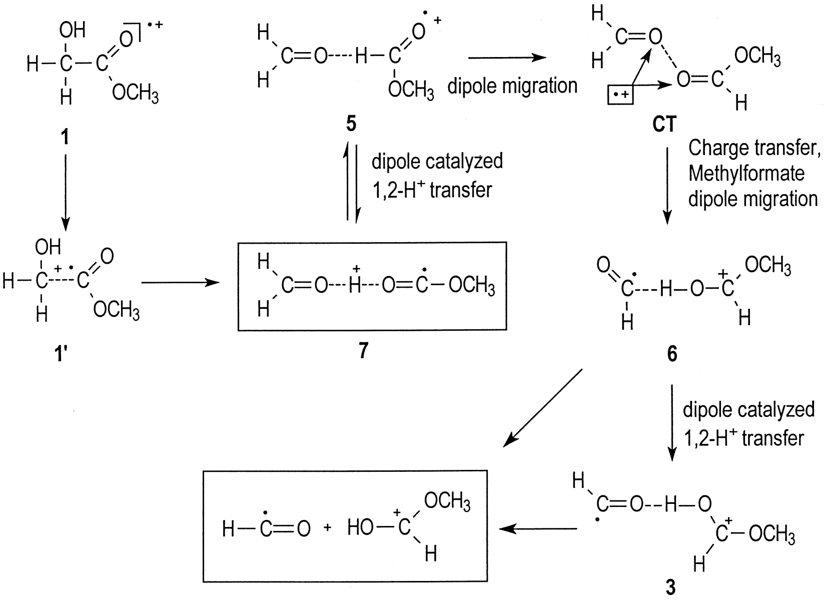

Scheme 3.

see Fig. 3, imposes a sizable energy barrier upon the isomerization **1** → **7** and because it also lies close to the dissociation threshold this may explain why the HBRC **7** does not significantly interconvert with **1** prior to dissociation. Thus we conclude that the dissociation route **1** → **7** → **D** is viable and Scheme 3 presents the new mechanism for the loss of HC=O$^{\cdot}$ from both ions **1** and **7**.

The second question involves the communication between the dimethylcarbonate ions **2** and the methylglycolate ions **1**. It is clear from the experimental observations on the labeled isotopomers that the original proposal from [1], i.e. **2** → **7** → **1** cannot be valid and moreover the new mechanism derived from our computations cannot accommodate such a proposal either.

How then do ions **2** communicate with **1** prior to their dissociation into $CH_3OC(H)OH^+ + HC{=}O^{\cdot}$? We note that both **1** and **2** have a great many isomers and conformers whose relative energies lie below the $\sim$12 kcal mol^{-1} limit imposed by experiment and several of these have been reported in [1]. However, the presence of such a large number of stable isomers and conformers makes the search for connecting transition states (TS) a truly formidable task. Moreover, as pointed out in Sec. 1 the elusive TS for **1** → **2** must be fairly high in energy (i.e. comparable to TS **1** → **7**) to accommodate the labeling results and this makes the search even more difficult.

One intuitive possibility is presented in Scheme 4. It represents a connection of **1** (via **8**) with **2** (via **9**) via a ring closed oxirane-type ion. Exploratory calculations indicate this ion could be a fairly high lying TS but whether it does represent the elusive connection between **1** and **2** must be studied further and results will be reported in a future publication.

3. Theoretical methods

The computational results reported in this study were obtained at the UCCSD(T)/cc-pVDZ//UMP2(Full)/6-31G** + ZPVE level of theory using the GAUSSIAN94 and GAMESS computational packages [15,16]. The coupled cluster approximation [17] utilizing singles, doubles, and estimated triple excitations [CCSD(T)] was used to obtain our best relative energies on UMP2(Full)/6-31G** optimized structures. The

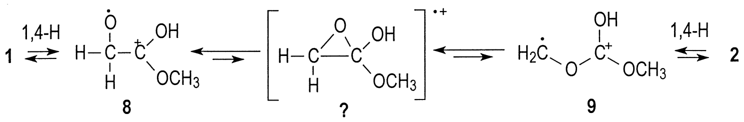

Scheme 4.

CCSD(T) calculations used the double zeta correlation consistent basis set of Dunning, cc-pVDZ [18]. All transition states had the correct number of negative eigenvalues of the corresponding Hessian matrix. The spin contamination of the UHF wavefunctions was acceptable for all species investigated, i.e. less than 10% of 0.75. The calculations are summarized in Table 1 and Figs. 2 and 3. Table 1 presents the ZPVEs, theoretical relative energies, and experimental relative energies for the isomers and some important dissociation products. All relative energies were calculated relative to the dissociation limit of the reaction studied, viz. $CH_3OC(H)OH^+ + HC{=}O^{\cdot}$ (**D**) for which reliable experimental energies are also available. Based on the results from the previous study we expect that the uncertainty in the relative energies derived from the computational procedure is about 3 kcal mol^{-1} [1]. Fig. 2 presents the optimized geometries of the minima, transition states, and the charge transfer complex for the key isomers along the reaction path. The reaction pathways were verified with IRC calculations [15], and in regions of correct PES curvature, the eigenvalue-following [19] routine was used to find the stationary points, as indicated with (EF) in Fig. 2. Fig. 3 presents a combined experimental and theoretical energy level diagram for the loss of $HC{=}O^{\cdot}$ from both ions **1** and **7**.

4. Experimental methods

The mass spectrometric experiments were performed with the McMaster University VG Analytical (Manchester, UK) ZAB-R instrument of BE_1E_2 geometry (B, magnet; E, electric sector) [20] using an accelerating voltage of 8 or 10 keV. Metastable ion (MI) mass spectra were recorded in the second field-free region (2ffr); CID mass spectra were recorded in the 2 and 3ffr using oxygen as collision gas (transmittance $T = 70\%$). The CID mass spectra of the 2ffr metastable or CID peaks (MS/MS experiments) were obtained in the 3ffr using O_2 as the collision gas. All spectra were recorded using a small PC-based data system developed by Mommers Technologies Inc. (Ottawa, ON). The DMO samples used in this study were obtained from Aldrich and used without further purification.

Acknowledgements

J.K.T. thanks the Natural Sciences and Engineering Research Council of Canada (NSERC) for financial support. P.J.A.R. thanks the Netherlands Organization for Scientific Research (NWO) for making available the Cray-YMP of SARA (Amsterdam) through the Netherlands Foundation for Chemical Research (SON).

References

[1] L.M. Fell, P.C. Burgers, P.J.A. Ruttink, J.K. Terlouw, Can. J. Chem. 76 (1998) 335.

[2] D. Suh, C.A. Kingsmill, P.J.A. Ruttink, P.C. Burgers, J.K. Terlouw, Int. J. Mass Spectrom. Ion Processes 146/147 (1995) 305.

[3] D. Suh, P.C. Burgers, J.K. Terlouw. Rapid Commun. Mass Spectrom. 9 (1995) 862.

[4] (a) P.J.A. Ruttink, P.C. Burgers, J.K. Terlouw, Can. J. Chem. 74 (1996) 1078; (b) P.J.A. Ruttink, P.C. Burgers, Org. Mass Spectrom. 28 (1993) 1087; (c) P.J.A. Ruttink, P.C. Burgers, L.M. Fell, J.K. Terlouw, J. Phys. Chem. A 102 (1998) 2976; (d) T.H. Morton, Tetrahedron 38 (1982) 3195. See also the following: T.H. Morton, Org. Mass Spectrom. 27 (1992) 353; H.W. Biermann, T.H. Morton, J. Am. Chem. Soc. 105 (1983) 5025.

[5] (a) S. Lias, J.E. Bartmess, J.F. Liebman, J.L. Holmes, R.D. Levin, W.G. Mallard, J. Phys. Chem. Ref. Data 17 (1988) (suppl. 1); E.P. Hunter, S.G. Lias, J. Phys. Chem. Ref. Data 27 (1998) No. 3; see also NIST Chemistry WebBook, http://

webbook.nist.gov/chemistry/; (b) J.C. Traeger, B.M. Kompe, in J.A.M. Simões, A. Greenberg, J.F. Liebman (Eds.), Energetics of Organic Free Radicals, Blackie Academic & Professional, New York, 1996, Chap. 3; (c) L.M. Fell, P.C. Burgers, P.J.A. Ruttink, J.K. Terlouw, J. Phys. Chem. A 103 (1999) 1426; (d) J.E. Szulejko, T.B. McMahon, J. Am. Chem. Soc. 115 (1993) 7839.

[6] M.A. Trikoupis, J.K. Terlouw, P.C. Burgers, M. Peres, C. Lifshitz, J. Am. Soc. Mass Spectrom. 10 (1999) 869 and references cited therein.

[7] J.L. Holmes, F.P. Lossing, P.M. Mayer, J. Am. Chem. Soc. 113 (1991) 9723.

[8] (a) W.V. Steele, R.D. Chirico, S.E. Knipmeyer, A. Nguyen, N.K. Smith, J. Chem. Eng. Data 41 (1996) 1285; (b) W.V. Steele, R.D. Chirico, S.E. Knipmeyer, A. Nguyen, N.K. Smith, J. Chem. Eng. Data 42 (1997) 1037.

[9] B.J. Smith, L. Radom, J. Phys. Chem. 99 (1995) 6468.

[10] M. Meot-Ner (Mautner), J. Am. Chem. Soc. 106 (1984) 1257 and using the appropriate ΔH_f values from [4].

[11] (a) N. Heinrich, T. Drewello, P.C. Burgers, J.C. Morrow, J. Schmidt, W. Kulik, J.K. Terlouw, H. Schwarz, J. Am. Chem. Soc. 114 (1992) 3776; (b) J.K. Terlouw, J. Wezenberg, P.C. Burgers, J.L. Homes, Chem. Commun. (1983) 1121; (c) W. Bertrand, G. Bouchoux, Rapid Commun. Mass Spectrom. 12 (1998) 1697.

[12] (a) A.J. Chalk, L. Radom, J. Am. Chem. Soc. 119 (1997) 7573; (b) J.W. Gauld, H. Audier, J. Fossey, L. Radom, J. Am. Chem. Soc. 118 (1996) 6299; (c) J.W. Gauld, L. Radom, J. Am. Chem. Soc. 119 (1997) 9831.

[13] (a) D.K. Bohme, Int. J. Mass Spectrom. Ion Processes 115 (1992) 95; (b) P. Mourges, H.E. Audier, D. Leblanc, S. Hammerum, Org. Mass Spectrom. 28 (1993) 1098; (c) H.E. Audier, D. Leblanc, P. Mourges, T.B. McMahon, S. Hammerum, J. Chem. Soc. Chem. Commun. (1994) 2329; (d) H.E. Audier, J. Fossey, P. Mourgues, T.B. McMahon, S. Hammerum, J. Chem. Phys. 100 (1996) 18 390.

[14] P.C. Burgers, L.M. Fell, A. Milliet, M. Rempp, P.J.A. Ruttink, J.K. Terlouw, Int. J. Mass Spectrom. Ion Processes 167/168 (1997) 291.

[15] J.B. Foresman, A. Frisch, Exploring Chemistry with Electronic Structure Methods, Gaussian, Pittsburgh, 1996.

[16] (a) M.J. Frisch, G.W. Trucks, H.B. Schlegel, P.M.W. Gill, B.G. Johnson, M.A. Robb, J.R. Cheeseman, T.A. Keith, G.A. Peterson, J.A. Montgomery, K. Raghavachari, M.A. Al-Laham, V.G. Zakrevski, J.V. Ortiz, J.B. Foresman, C.Y. Peng, P.Y. Ayala, W. Chen, M.W. Wong, J.L. Andres, E.S. Replogle, R. Gomperts, R.L. Martin, D.J. Fox, J.S. Binkley, D.J. de Frees, J. Baker, J.P. Stewart, M. Head-Gordon, C. Gonzales, J.A. Pople, GAUSSIAN 94, Revision B.3, Gaussian Inc., Pittsburgh PA, 1995; (b) M.F. Guest, J. Kendrick, GAMESS Users Manual, SERC Daresbury Laboratory, CCP/86/1, 1986; M. Dupuis, D. Spangler, J. Wendolowski, NRCC Software Catalog, Vol. 1, Program No. QG01 (GAMESS), 1980; (c) M.F. Guest, R.J. Harrison, J.H. van Lenthe, L.C.H. van Corler, Theor. Chim. Acta 71 (1987) 117.

[17] (a) J. Cizek, Adv. Chem. Phys. 14 (1969) 35; (b) J.A. Pople, R. Krishnan, H.B. Schlegel, J.S. Binkley, Int. J. Quant. Chem. 14 (1978) 545; (c) R.J. Bartlett, G.D. Purvis, Int. J. Quant. Chem. 14 (1978) 516.

[18] (a) T.H. Dunning Jr., J. Chem. Phys. 90 (1989) 1007; (b) R.A. Kendall, T.H. Dunning Jr., R.J. Harrison, J. Chem. Phys. 96 (1992) 6796.

[19] M.J. Frisch, A.E. Frisch, J.B. Foresman, GAUSSIAN 94 User's Reference, 2nd ed., Pittsburgh, 1996.

[20] H.F. van Garderen, P.J.A. Ruttink, P.C. Burgers, G.A. McGibbon, J.K. Terlouw, Int. J. Mass Spectrom. Ion Processes 121 (1992) 159.